



Colorimetric and visual determination of acrylamide via acrylamide-mediated polymerization of acrylamide-functionalized gold nanoparticles

Xingbo Shi^{1,2} · Dai Lu¹ · Zimeng Wang¹ · Dong Zhang¹ · Wenli Gao¹ · Chunyan Zhang¹ · Jiehong Deng¹ · Shiyin Guo¹

Received: 9 July 2018 / Accepted: 19 October 2018 / Published online: 27 October 2018
© Springer-Verlag GmbH Austria, part of Springer Nature 2018

Abstract

A colorimetric assay is described for acrylamide (AA). It is based on color changes induced by an increase in the distance between gold nanoparticles (AuNPs) that is caused by AA copolymerization. First, AuNPs were modified with a thiolated propylene amide poly(ethylene glycol) that also contains the AA functionality. The carbon-carbon double bonds on the modified AuNPs can be polymerized under the catalysis of a photoinitiator and under UV irradiation. This results in the aggregation of the AuNPs and in a color change from red to gray. In the presence of AA, the distance between the AuNPs increases due to copolymerization with AA, and the solution of AuNPs preserves its original red color. Under optimized conditions, the absorption ratio (A_{525}/A_{740}) of the solution increases linearly in the 1 nM to 10 μ M free AA concentration range, with a 0.2 nM limit of detection. Hence, the method meets the need for rapid monitoring of trace AA in food. The method has a relative error (RSD) that is lower compared to the accepted HPLC method.

Keywords Colorimetry · Polymerization · Carbon-carbon double bonds · Thermally processed food · Food safety · Vinyl compounds · Photo-initiator

Introduction

Acrylamide (AA) has raised considerable attention after it was detected in many thermally processed food by the Swedish National Food Administration and Stockholm University in 2002 [1, 2]. After AA was classified as probably carcinogenic

to humans by the International Agency for Research on Cancer (IARC) in early 1994 [3], subsequent studies have found amounts of AA in thermally processed foods [4], such as crisps, biscuits, and coffee, which greatly exceed the limited value ($0.5 \mu\text{g L}^{-1}$) of AA in drinking water proposed by WHO [5].

For these years, researchers have investigated the inhibition of AA formation during food hot processing [6–9]. However, there are fewer reports on methods of AA detection. Even though, accurate quantitative analysis of AA in food is the prerequisite to study the formation mechanism and inhibition of AA. Because of its low molecular weight (71.08), high polarity and lack of obvious chromophoric group, the trace analysis of AA is particularly difficult [10, 11]. Therefore, it is important to develop a reliable, sensitive and selective method for on-site and real-time detection of AA in thermally processed food.

Current traditional detection methods for AA, such as GC (gas chromatography), LC (liquid chromatography), GC-MS (gas chromatography-mass spectrometry) and LC-MS (liquid chromatography-mass spectrometry) [12–15], all require sophisticated instrumentation and professional operation, making on-site and real-time AA analysis difficult.

Electronic supplementary material The online version of this article (<https://doi.org/10.1007/s00604-018-3062-5>) contains supplementary material, which is available to authorized users.

✉ Xingbo Shi
shixingbo123@aliyun.com

✉ Jiehong Deng
hongjiedeng@163.com

✉ Shiyin Guo
gsy@hunau.edu.cn

¹ Hunan Provincial Key Laboratory of Food Science and Biotechnology, College of Food Science and Technology, Hunan Agricultural University, Changsha 410128, China

² State Key Laboratory of Chemo/Biosensing and Chemometrics, Hunan University, Changsha 410082, China

Several new methods have been developed, such as capillary electrophoresis (CE) [16], enzyme-linked immunosorbent assay (ELIAS) [17], electrochemical analysis [18] and AA-derivatization fluorescence approach [19]. But, they still require cumbersome pretreatment procedures, which preclude on-site applications. In 2014, a potential nano-biosensing method [20] for AA detection has emerged. Hu et al. [20] reported a novel fluorescent sensing method for AA detection based on AA polymerization-induced distance increase between quantum dots, with a limit of detection of $3.5 \times 10^{-5} \text{ g}\cdot\text{L}^{-1}$. However, the sensitivity is not comparable to that of traditional LC-MS/MS analysis, and is not unsuitable for the determination of low concentration of AA in food. Thus, a highly-sensitive, rapid and cost-effective strategy for the detection of AA is still challenging.

Colorimetric methods, in particular those based on the aggregation and re-dispersion of gold nanoparticles (AuNPs) [21], are extremely attractive because of these bare-eye visible signal readout, rapid response, cost-effective methods, and their freedom from instrumentation requirements. They have been used in a variety of forms for the detection of DNA [22], proteins [23], ions [24, 25], small molecules [26–28], cancer cells [29] and virus [30]. The key point designing a new colorimetric method is how to trigger a distance change between AuNPs. Initiation is commonly based on bio-recognition such as immune-recognition, DNA hybridization and aptamer response, or on physical interactions such as electrostatic and steric effects. But, lack of those properties for AA makes it difficult to design a colorimetric method for detecting AA.

In this study, a novel colorimetric method for the detection of AA was developed based on AA-mediated polymerization to induce a distance increase between AuNPs. We firstly utilized thiolated propylene amide poly (ethylene glycol) (AA-PEG-SH) to modify AuNPs as a probe. The carbon-carbon double bonds of the AA component of AA-PEG-SH can be polymerized with the help of UV photo initiator, resulting in a decrease in the distance between AuNPs and a color change from red to gray. In the presence of AA, the distance between AuNPs becomes greater due to copolymerization of free AA, with the color returning to original state. The new colorimetric strategy was employed to detect AA in a variety of food samples with excellent linear range, low cost, and good sensitivity.

Material and methods

Reagents and apparatus

Chloroauric acid ($\text{HAuCl}_4 \cdot 3\text{H}_2\text{O}$), trisodium citrate, potassium bromide, ethanol, hydrochloric acid, nitric acid, acetic acid, maleic acid, caffeic acid, fumaric acid, acrylic acid, propionic acid, butyric acid, cinnamic acid and potassium sorbate, were purchased from Sinopharm Chemical Reagent Co.,

Ltd.(Shanghai, China, www.sinopharm.com). Diphenyl (2,4,6-trimethylbenzoyl) phosphine oxide (TPO), L-asparagine and AA were purchased from Sigma-Aldrich (www.sigmaaldrich.com). AA-PEG-SH was purchased from Shanghai Ponsure Biotech, Ltd. (Shanghai, China, www.ponsure.cn). Ultrapure water ($18.2 \text{ M}\Omega\cdot\text{cm}$) was prepared using a milliQ purification-system (Millipore USA, www.merckmillipore.com).

The polymerization reaction was induced by a UV Transmission Analyzer (WFH-204B, Shanghai Chi Tang electronics Co., Ltd., www.cit17.com). UV-vis spectra of AuNPs were obtained by an UV-2450 Spectrophotometer(Shimadzu Co., Ltd., Japan, www.shimadzu.com.cn).The AuNPs modified with AA-PEG-SH were characterized by Fourier Transform Infrared Spectrometry (IR Affinity-1, Shimadzu Enterprise Management Co., Ltd., China, www.shimadzu.com.cn). Transmission electron microscopic (TEM) images were recorded with a JEM-2100 (JEOL, Tokyo, Japan, www.jeol.co.jp). Particle size and zeta potential were measured by a Zetasizer Nano-ZS90 (Malvern Instruments Ltd., www.malvernpanalytical.com). The content of AA in food was analyzed by a Waters e2695 HPLC (Milford, Massachusetts, USA, www.waters.com).

Synthesis of AuNPs

We first prepared the seed AuNPs with a mean diameter of 16.8 nm by a method published previously [31, 32]. In brief, 0.6 mL trisodium citrate (0.2 mM) solution was added to 100 mL of boiling HAuCl_4 (2.428 mM) solution, and consistently stirred for an additional 20 min until the color of the mixture turned from light yellow to wine red. To increase the surface plasmon resonance absorption peak of AuNPs, larger size of AuNPs was further synthesized. The solution, containing 5 mL of seed AuNPs, 0.3 mL of HAuCl_4 (24.28 mM) solution and 35 mL of ultrapure water, was reduced by 0.15 mL of trisodium citrate (13 mM) at 120°C for 20 min. Until the color changed to wine red, indicating the formation of larger size AuNPs. The diameter of resultant AuNPs was determined by TEM, and found to be $27.93 \pm 1.93 \text{ nm}$. The concentration of the AuNPs (0.372 nM) was calculated by the absorbance measurements based on an extinction coefficient of $1.58 \times 10^9 \text{ M}^{-1} \text{ cm}^{-1}$ at wavelength of 450 nm [33]. Finally, the AuNP solution was stored at 4°C in the dark, and used it in the subsequent experiments.

Preparation of AA-PEG-SH modified AuNPs

Thirty microliters AA-PEG-SH solution (0.5 mM) was slowly added to 5 mL AuNP solution. Then this mixture was stirred at 45°C overnight (12 h). The AA-PEG-SH formed a strong link with AuNPs by strong covalent bonding between AuNPs and the group -SH. Unreacted AA-PEG-SH was removed by

centrifuging at 4000 rpm for 10 min and washing 3 times with doubly-distilled water and centrifugation. After removing the supernatant, the AA-PEG-AuNP was quickly diluted by doubly-distilled water under the assist of ultrasound and kept the volume of solution at 5 mL. Therefore, the concentration of resultant AA-PEG-AuNP solution was still 0.372 nM. Before using it, this solution was filtered through a microporous membrane of 0.45 μm and stored at 4 $^{\circ}\text{C}$.

Detection of AA in aqueous solutions

During colorimetric detection, 0.4 mL of different concentrations of AA (1×10^{-5} , 1×10^{-6} , 1×10^{-7} , 1×10^{-8} , 5×10^{-9} , 1×10^{-9} M) standard solutions were added to 3.6 mL of AA-PEG-AuNPs solution, followed by addition 4 mM TPO, to make the TPO concentration of the mixture solution 1 mmol L^{-1} . After 16 min UV illumination, the absorbance was recorded by a UV-vis spectrophotometer in the range of 300–900 nm, and the corresponding images were obtained by a mobile camera. All the measurements were repeated 3 times for each sample.

To determine the specificity of the method, 3.6 mL of AA-PEG-AuNP solution containing 1 mmol L^{-1} TPO was spiked with 0.25 mM of 10 different compounds similar to AA in chemical structure, including acetic acid, maleic acid, caffeic acid, fumaric acid, acrylic acid, propionic acid, butyric acid, L-asparagine, cinnamic acid and potassium sorbate. The absorption intensity and the color images of these solutions were separately monitored under the same conditions as the AA detection.

Detection of AA in real sample

In order to investigate the potential applicability of the colorimetric method to real samples, detection of AA was carried out in potato chips, cookies and non-fried cookies. For real sample pretreatment, potato chips, cookies and non-fried cookies which were purchased from a local supermarket, were crushed into powder with a mortar. A portion of 2.5 ± 0.10 g was weighed into a 50 mL centrifugal tube, and was dissolved in 25 mL ultrapure water. The mixture was sonicated for 20 min to extract the AA. In order to remove the protein, 1 mL of 106 g L^{-1} potassium ferricyanide solution and 1 mL of 219 g L^{-1} zinc acetate solution were added. After 10 min, the mixture was filtered with a qualitative filter. In this process, the mixture was eluted three times by using ultrapure water and then collected 30 mL solution. Finally, the filtrate solution was filtered through 0.45 μm membranes before its detection.

To evaluate the accuracy of the colorimetric strategy, HPLC analysis was performed using a standard method on a Waters e2695 HPLC system equipped with an e2998 diode array detector. Chromatographic separation was performed on

a symmetry-C18 column (4.6 mm \times 250 mm, 5.0 μm). Ten microliters of sample solution was injected into the HPLC system, and then eluted using 10% methanol in water at a flow rate of 0.8 mL/min at 30 $^{\circ}\text{C}$. The concentration of AA was detected by monitoring the 197 nm absorption peak. All mobile phases were degassed prior to injection by using an ultrasonicator (KQ3200E, Kunshan Ultrasonic Instrument Co., Ltd) and were filtered through 0.45 μm membranes. A series of concentrations of AA (1, 5, 10, 15, 20 $\mu\text{mol L}^{-1}$) was measured to obtain a standard curve. The concentrations of AA formation in the reaction solution were calculated using the standard curve.

Results and discussion

Principle of the colorimetric strategy

The detection principle of this colorimetric strategy is based on the polymerization of AA, causing the AuNPs to aggregate. As shown in Fig. 1, the functional molecule AA-PEG-SH, composed of an AA molecule, a PEG extenders and a sulfhydryl group, are modified on the surface of AuNPs through an Au-S covalent bond. The dispersed AA-PEG-AuNP solution shows a typical absorption peak at 525 nm and a wine red color. When the AA-PEG-AuNP solution is triggered by photo-initiator TPO under UV irradiation, the carbon-carbon double bonds in AA undergo addition polymerization and induce AuNP aggregation along with a color change. In the presence of AA, the free AA can copolymerize with the probe, leading to a greater distance between the AuNPs, and the color of the AuNP solution remains the same as that of the dispersed AA-PEG-AuNP solution.

Photoinitiation of AA copolymerization

Because poly-acrylamide can be characterized by a broad absorption from 450 to 700 nm, we utilized UV-vis spectra of poly-acrylamide to estimate the degree of polymerization. The results (Figure S1, A, B) show that the polymerization of AA is easily triggered by photo-initiator TPO. The amount of TPO is a key of factor in the polymerization. To optimize the concentration of TPO for the subsequent experiments, different concentrations of TPO were added to 100 mmol L^{-1} AA solutions. According to the results (Figure S1, C, D), 1 mmol L^{-1} TPO was chosen for subsequent experiment, which is also similar with the Hu group's result [20].

Feasibility of the detection principle

Successful modification of AA-PEG-SH on the surface of AuNPs is a critical step to exploit the colorimetric strategy. To verify the modification of AuNPs with AA-PEG-SH, pure

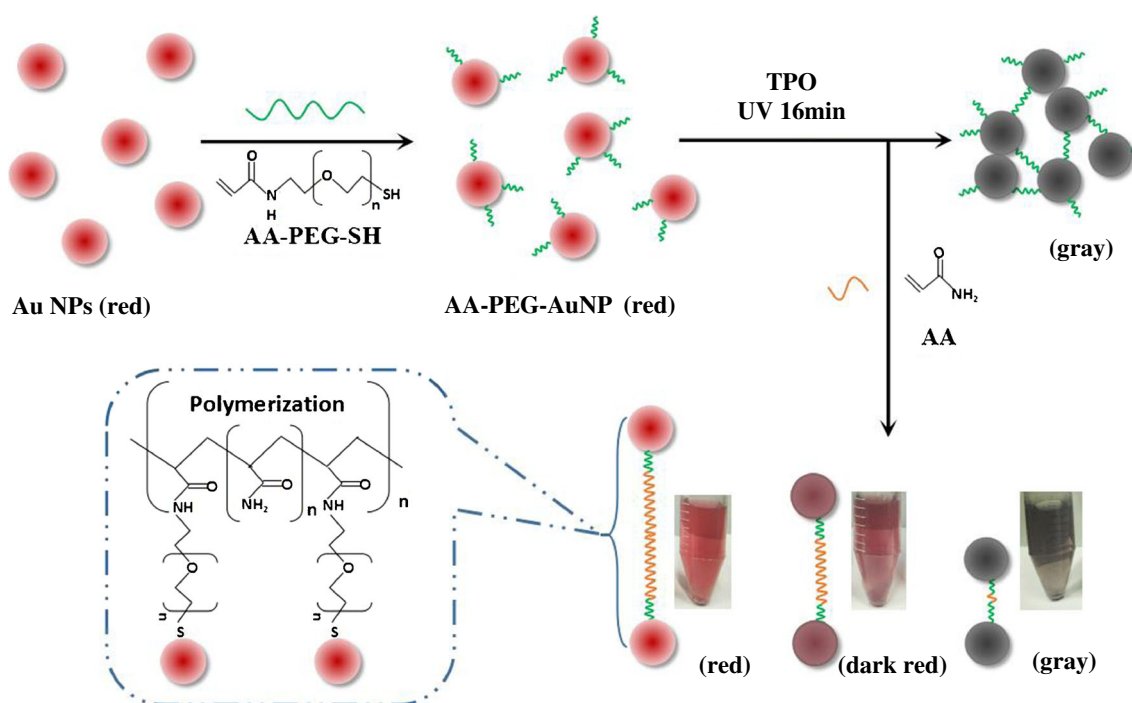


Fig. 1 Schematic illustration of the colorimetric strategy for AA detection using the AA-PEG-AuNP. AA-PEG-SH, as functional molecule, was modified on the surface of bare AuNPs. The functionalized AuNPs (AA-PEG-AuNP) were used to detect AA based on the color changes of

AuNP solution with AA and without AA due to copolymerization of AA inducing the distance increase between AuNPs under the catalysis of the photo-initiator TPO and UV irradiation

AuNPs, AA-PEG-SH and functional AuNPs (AA-PEG-AuNP) were characterized by FT-IR spectroscopy (Fig. 2b). Comparing AA-PEG-AuNP with AuNPs, the transmission of $-\text{CH}=\text{CH}-$ (669 cm^{-1}), $-\text{CH}_2-$ ($2840\text{--}2930\text{ cm}^{-1}$), $-\text{C}=\text{O}-$ (1753 cm^{-1}) increases after reaction, demonstrating that AA-PEG-SH has been modified on the surface of AuNPs. Zeta-potential measurements also verified the modification. In Fig. 2c, the Zeta-potential of pure AuNPs is -28.18 mV , which is similar to the value in the previous report [34]. But, the AA-PEG-AuNP present positive charge in Zeta-potential measurements, which attributed to the modification with the AA-PEG-SH.

To further confirm the detection principle, the dispersion of AuNPs in different conditions was evaluated by UV-vis spectroscopy, IR spectroscopy, Zeta potential and TEM. As shown in Fig. 2a, a characteristic surface plasmon resonance (SPR) band of the pure AuNPs was observed in the spectrum at approximately 525 nm , but the modified AuNP (AA-PEG-AuNP) solution shows a small change in absorbance and color in comparison with pure AuNP solutions. After the addition of TPO and irradiation with UV, the color of AuNP solutions changes from red to gray (Fig. 2a inset images), and a strong absorption peak at 740 nm appears, indicating serious aggregation of AuNPs. The aggregation of AuNPs was further evidenced by TEM images that revealed well dispersed AuNPs in the absence of TPO (Fig. 2d, e) and significant aggregation in the presence of TPO (Fig. 2f). The transmission of $-\text{CH}=\text{CH}-$

$-\text{CH}=\text{CH}-$ (669 cm^{-1}) in the FT-IR spectrum vanishes (Fig. 2b, dark green line) and the Zeta-potential of AA-PEG-AuNP returns to a negative value (Fig. 2c), both effects indicating that polymerization between $-\text{CH}=\text{CH}-$ groups on the surface of AuNPs occurred.

Optimization of parameters

In addition to TPO concentration, the concentration of AA-PEG-SH and the reaction time also play important roles in the polymerization reaction. For the optimization of AA-PEG-SH concentration, we added different concentration ($0, 2.4, 3.0, 3.6, 4.2, 4.8, 5.4$ and $6.0\text{ }\mu\text{M}$) of AA-PEG-SH to modify the AuNPs. After reaction in the dark for 12 h, the mixture was observed by UV-Vis spectrophotometry. Figure S2 shows the interaction between AuNPs and different concentration of AA-PEG-SH. Interestingly, the main absorption peak at 525 nm decreased gradually, and new absorption peaks appeared and shifted from 650 to 740 nm with increasing AA-PEG-SH concentration from 0 to $6\text{ }\mu\text{M}$. The corresponding color of the AuNP solution changed from red to purple and then gray. These results indicate that adding more AA-PEG-SH can induce AuNPs self-aggregation, even without photo-initiator TPO. Considering the stability for the functional AuNP solution and the sensitivity of the colorimetric strategy, $3\text{ }\mu\text{M}$ was chosen as the optimized AA-PEG-SH concentration, because the color of AuNP solution (as shown in

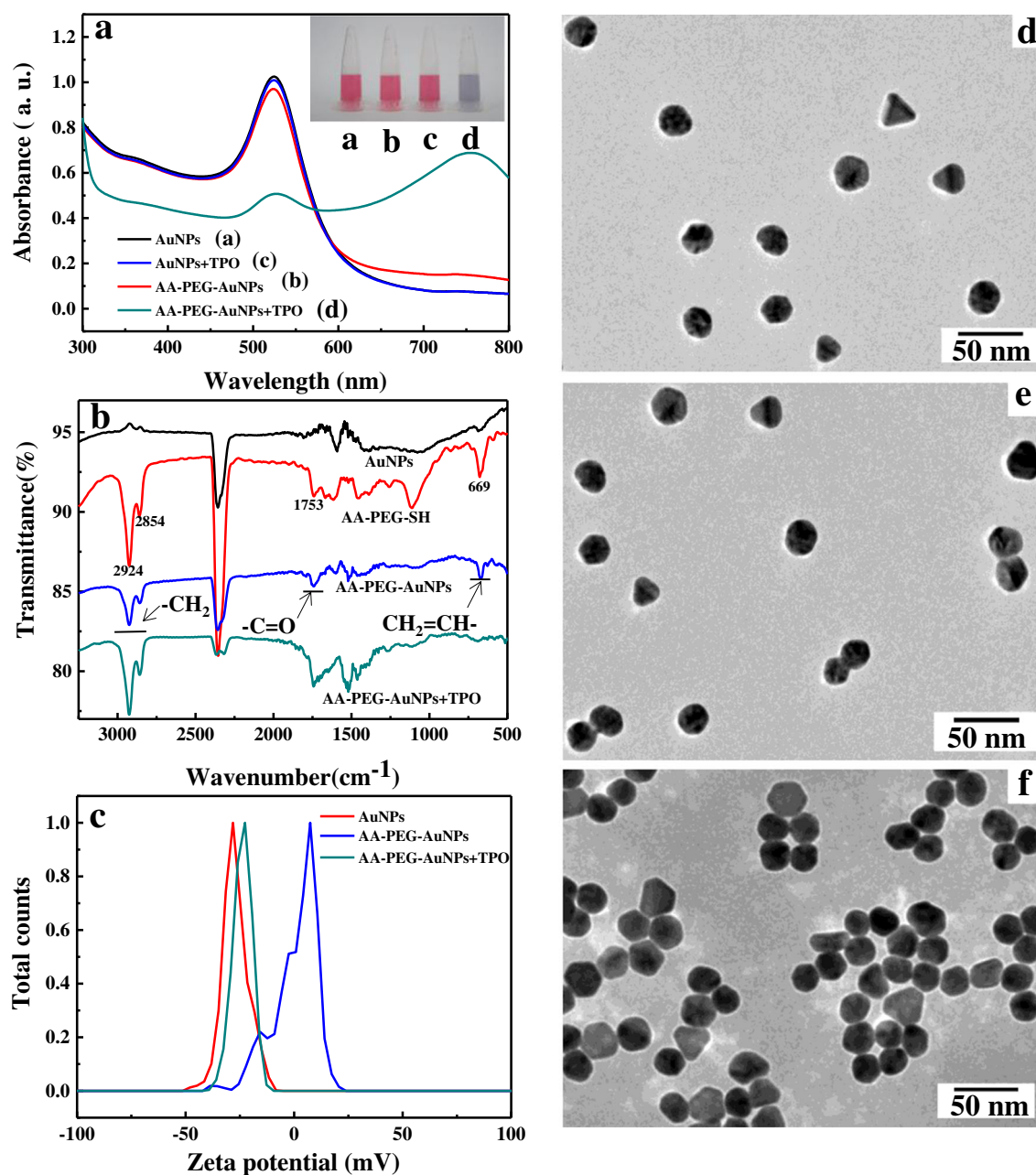


Fig. 2 **a** Confirmation of the detection principle by UV-vis absorption spectra, inset: photograph of AuNPs with different treatments; **b** FT-IR spectra of bare AuNPs, AA-PEG-SH, AA-PEG-AuNP and AA-PEG-AuNP after addition of the photo-initiator TPO and UV irradiation. **c** The

zeta-potential of bare AuNPs, AA-PEG-AuNP and AA-PEG-AuNP after TPO catalysis. **(d-f)** Typical TEM images of bare AuNPs **(d)**, AA-PEG-AuNP without **(e)** and with **(f)** TPO catalysis

Figure S2 inset images) changed only slightly with addition of 3 μ M AA-PEG-SH compared to the pure AuNP solution.

The reaction time is other important parameters in the polymerization, which is a continuous reaction. Because polymerization induces the AuNPs aggregation, observing the color change or measuring the absorbance change can be used to monitor process of the polymerization reaction. Figure S3A shows the change of A_{525}/A_{740} ratio of AA-PEG-AuNP solution triggered by TPO with increasing reaction time. There is rapid decrease in the ratio at beginning of reaction, but a

plateau is reached after 16 min. To further confirm whether the addition of AA will influence the rate of polymerization, we also examined the change of the A_{525}/A_{740} ratio with the addition of 10 mM free AA group (as shown in Figure S3B). The tendency is similar to that without AA, but the magnitude of the change is much greater. Considering the time efficiency, 16 min was chosen as the optimal final reaction time in the subsequent experiments. In addition, the stability of AA-PEG-AuNP probe without triggered by TPO was examined. Figure S4 shows the spectra (Figure S4A) and A_{525}/A_{740}

values (Figure S4B) of AA-PEG-AuNP probe solution slightly change with different incubation time (24 h, 48 h, 72 h, 96 h, 120 h, 144 h, 168 h), indicating that incubation time didn't obviously affect the stability of AA-PEG-AuNP probe and the influence may be ignorable.

Sensitivity of the colorimetric strategy

Under the above-mentioned optimized detection conditions, the sensitivity of the method to AA was investigated by interaction of the AA-PEG-AuNP solution with different concentrations of AA standard solutions in the presence of photoinitiator (TPO) and UV-irradiation. Upon increasing AA concentration, the absorbance at 525 nm gradually decreased, while an increase in the absorption at 740 nm can be observed (Fig. 3a). This indicates that the AA-PEG-AuNP induces aggregation at low AA concentration, and the corresponding color of AA-PEG-AuNP gradually turned from red to purple (Fig. 3a inset). The A_{525}/A_{740} value of AA-PEG-AuNP increased gradually with increasing AA concentration. A good linear relationship between A_{525}/A_{740} and AA concentration was fitted by the regression equation $A_{525}/A_{740} = 0.89953 \lg[\text{AA}] + 9.29682$ with $R^2 = 0.99548$ (Fig. 3c). The limit of detection (LOD) was estimated to be 0.2 ± 0.028 nM based on the $3\sigma/S$ calculation (σ is the standard deviation for a blank solution and S is the slope of the calibration curve), which is lower than other reported value, as shown in Table S1. Figure 3b shows that the A_{525}/A_{740} value of the bare AuNP solution changes very slightly with different concentration of AA. This indicated that the bare AuNPs without modification with active AA-PEG-SH molecules cannot be used in the determination of AA.

Specificity of the AA sensing strategy

To investigate whether the colorimetric strategy is specific for AA detection, the selectivity was explored using various compounds, including acetic acid, maleic acid, caffeic acid, fumaric acid, acrylic acid, propionic acid, butyric acid, L-asparagine, cinnamic acid and potassium sorbate. As shown in the inset images of Fig. 4, significant color changes were observed only in the presence of AA. The color of the AA-PEG-AuNP in the presence of the other 10 compounds was gray or purple, approaching the color of the blank sample. The A_{525}/A_{740} ratio of the AA-PEG-AuNP system upon addition of AA was much higher than the ratio for the other 10 compounds (Fig. 4), which further indicates that this colorimetric strategy shows good selectivity for the detection of AA. The reason why the method has good selectivity against other 10 compounds is based on the principle of vinyl compounds polymerization [35]. Because the compounds, 1, 2 double substituents vinyl monomer ($\text{CHX}=\text{CHY}$, X and Y represent substituents) and three or four substituents ($\text{CX}_1\text{Y}=\text{CHX}_2$,

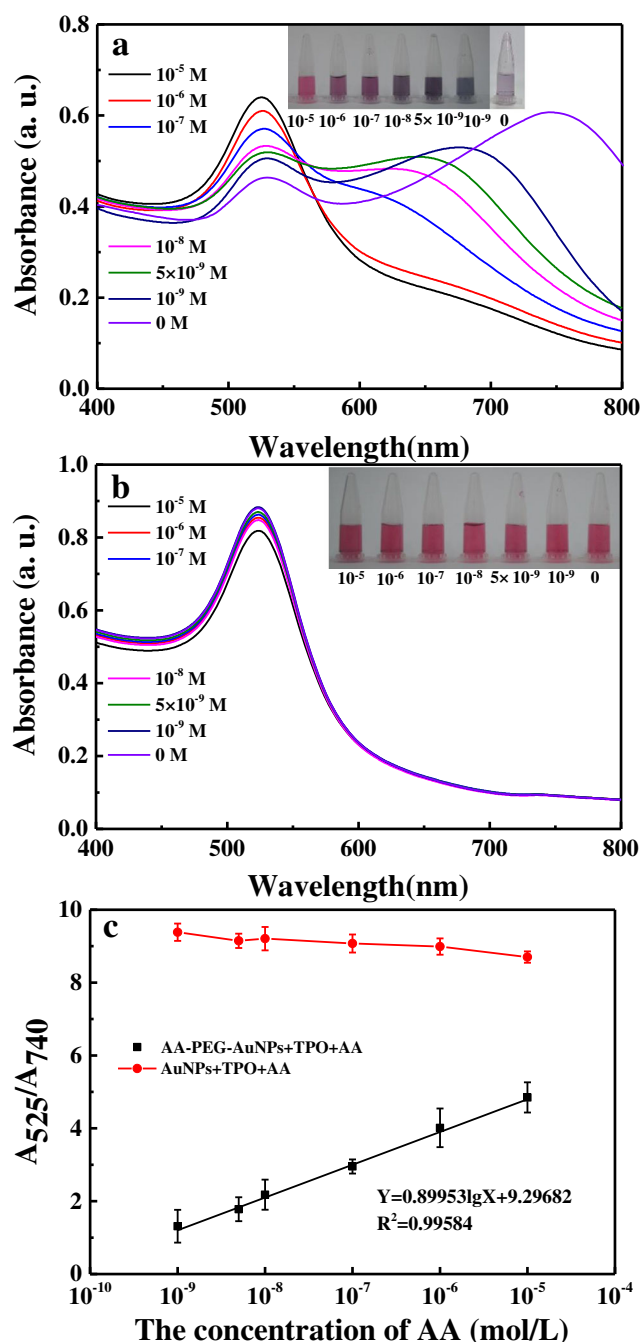


Fig. 3 UV-vis spectra of AA-PEG-AuNP (a) and bare AuNPs (b) with different concentrations of AA (1×10^{-5} , 1×10^{-6} , 1×10^{-7} , 1×10^{-8} , 5×10^{-9} , 1×10^{-9} , and 0 M). Inset: photographs of AA-PEG-AuNP with corresponding color visibly changed in the presence of different concentrations of AA. **c** Plots of A_{525}/A_{740} ratio of AA-PEG-AuNP and bare AuNPs versus the concentration of AA from 1×10^{-9} to 1×10^{-5} M. All the experiments were performed in the presence of 1 mmol L^{-1} TPO and under UV irradiation for 16 min

$\text{CX}_1\text{Y}_1 = \text{CX}_2\text{Y}_2$), cannot be polymerized owing to high steric hindrance. While fumaric acid, caffeic acid, maleic acid cinnamic acid and potassium sorbate are 1, 2 double substituents vinyl compounds, and all of them are also common food additives. For Acrylic acid, the A_{525}/A_{740} value exceed that of

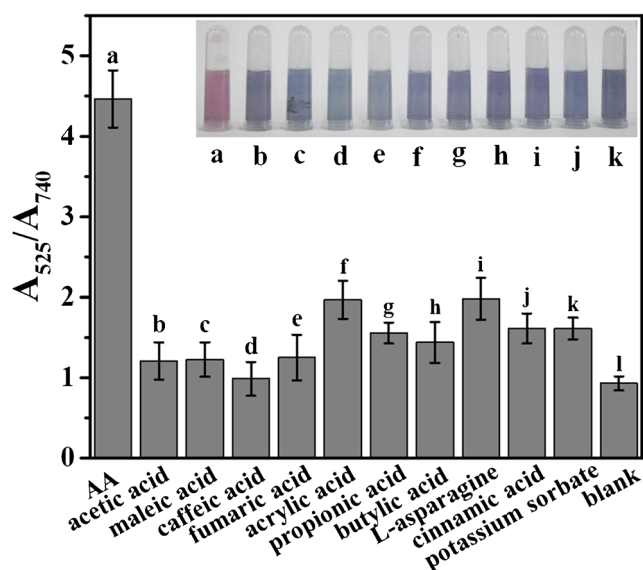


Fig. 4 Selectivity assay of the colorimetric method toward (a) 2.5 μM AA, (b) 0.25 mM acetic acid, (c) 0.25 mM maleic acid, (d) 0.25 mM caffeic acid, (e) 0.25 mM fumaric acid, (f) 0.25 mM acrylic acid, (g) 0.25 mM propionic acid, (h) 0.25 mM butyric acid, (i) 0.25 mM L-asparagine, (j) 0.25 mM cinnamic acid, (k) 0.25 mM potassium sorbate, (l) blank sample. Inset: the corresponding photograph of AA-PEG-AuNP in the presence of the other 10 compounds and AA

other control sample, is accordance with common principle, because it belongs to single substituent vinyl monomer ($\text{CH}_2 = \text{CHX}$), which can be polymerized in theory. However, it cannot influence AA detection in actual sample due to 100-fold concentration of control sample in comparison of AA.

Practical applicability of the colorimetric strategy

Considering the excellent selectivity, as well as the superior sensitivity, of this colorimetric strategy toward AA, the practical applicability of this method was further explored. First, several aqueous samples were prepared by spiking different concentrations (0 , 1×10^{-9} , 1×10^{-8} , 1×10^{-7} , 1×10^{-6} , 1×10^{-5} M) of standard AA solutions. As can be seen from Table 1, the recovery of added AA was in the range of 98.8 to 109.1%, which indicates that the established colorimetric strategy can be applied to accurately detect AA in aqueous samples with excellent reliability and reproducibility. In addition to the aqueous sample assay, we applied this colorimetric method to determine AA content in potato chips, baked cookies and non-fried cookies. The colorimetric determination of solution for real sample contains treated sample solution, colorimetric probes AA-PEG-AuNP and TPO initiator. In figure S5A is the absorption spectra of colorimetric determination of solution without UV irradiation. No obvious difference between the AA-PEG-AuNP solution and colorimetric determination of solution for the real sample was found, indicating that there was no effect of matrix on the assay. When the

Table 1 Recovery results for AA ($n = 3$) using our colorimetric strategy

Addition (mol/L)	Measured (mol/L)	SD	Recovery (%)
0	Not detected	—	—
1×10^{-9}	1.091×10^{-9}	1.42×10^{-10}	109.1
1×10^{-8}	1.067×10^{-8}	8.67×10^{-10}	106.7
1×10^{-7}	1.022×10^{-7}	1.48×10^{-8}	102.2
1×10^{-6}	0.988×10^{-6}	5.67×10^{-8}	98.8
1×10^{-5}	1.043×10^{-5}	2.17×10^{-6}	104.3

colorimetric determination of solutions were under the UV irradiation (figure S5B), the polymerization occurred accordingly, resulting in the change of absorption spectra of the solutions. This phenomenon is in accordance with the colorimetric principle. HPLC analysis was performed as a standard method to validate the accuracy of the new method again. In Table 2, it can be seen that the results performed by the established colorimetric strategy were in good agreement with those of the HPLC method, and with lower relative error (from 1.40% to 9.26%) suggesting that the colorimetric method can be applied to accurately detect AA in various foods.

Conclusions

In summary, a colorimetric method for AA detection was successfully developed based on AA-PEG-SH-modified AuNPs and AA polymerization. This method achieved a LOD of 0.2 ± 0.028 nM, which meets the need for rapid monitoring of trace AA in samples, and is far below the previously reported LODs obtained by other rapid detection methods. More importantly, this method does not require the use of any advanced and sophisticated instruments compared to other methods of AA detection. The new method was also employed to detect AA in real sample with satisfactory results compared with that of HPLC, thus providing a rapid and cost-effective method for determination of AA in hot processed foods. Definitely, this method may suffer from the average level of selectivity due to lack of any sensing agent. However, the key purpose to exploit this method only focus on food safety, the question of selectivity may be solved by

Table 2 The accuracy of colorimetric strategy in comparison with the HPLC method for the detection of AA in real samples

Samples	Content of AA based on two methods (mg/kg)		
	Colorimetric method	HPLC	Relative error
Baked cookies	5.86	5.779	1.40%
Potato chips	14.707	14.363	2.40%
Non-fried cookies	2.301	2.106	9.26%

elaborate pretreatment of food sample, since few of single substituent vinyl compounds can form in high temperature processing of food, except AA. In addition, the requirement of protection from light in the whole preparation process of AA-PEG-AuNP increases the risks of error and failure.

Acknowledgments The authors are grateful to the Natural Science Foundation of China (31301484), Natural Science Foundation of Hunan Province (2015JJ3082), Excellent Youth Foundation of Education Department of Hunan Province (17B124) and the Open Foundation of State Key Laboratory of Chemo/Biosensing and Chemometrics (Z2015025).

Compliance with ethical standards The author(s) declare that they have no competing interests.

References

- Mottram DS, Wedzicha BL, Dodson AT (2002) Acrylamide is formed in the Maillard reaction. *Nature* 419:448–449
- Stadler RH, Blank I, Varga N, Robert F, Hau J, Guy PA, Robert MC, Riediker S (2002) Acrylamide from Maillard reaction products. *Nature* 419:449–450
- (1994) IARC working group on the evaluation of carcinogenic risks to humans: some industrial chemicals. Lyon, 15–22. IARC Monogr Eval Carcinog Risks Hum 60:1–560
- Besaratinia A, Pfeifer GP (2007) A review of mechanisms of acrylamide carcinogenicity. *Carcinogenesis* 28(3):519–528
- WHO (2011) WHO/SDE/WSH/03.04/71/Rev/1
- Tran NL, Barraj LM, Collinge S (2017) Reduction in dietary acrylamide exposure-impact of potatoes with low acrylamide potential. *Risk Anal* 37:1754–1767
- Meghavarnam AK, Janakiraman S (2018) Evaluation of acrylamide reduction potential of l-asparaginase from *Fusarium culmorum* (ASP-87) in starchy products. *LWT Food Sci Technol* 89:32–37
- Wang ZM, Wen C, Shi XB, Lu D, Deng JH, Deng FM (2017) Simultaneous inhibition of acrylamide and hydroxymethylfurfural formation by sodium glutamate microcapsules in an asparagine-glucose model system. *J Food Sci Technol* 54:572–577
- Wen C, Shi XB, Wang ZM, Gao WL, Jiang LW, Xiao Q, Liu X (2016) Effects of metal ions on formation of acrylamide and 5-hydroxymethylfurfural in asparagine-glucose model system. *Inter J Food Sci Technol* 51:279–285
- Kim SH, Hwang JH, Lee KG (2011) Analysis of acrylamide using gas chromatography-nitrogen phosphorus detector (GC-NPD). *Food Sci Biotechnol* 20:835–839
- Shankar SS, Swamy BEK, Pandurangachar M, Chandra U, Chandrashekar BN, Manjunatha JG, Sherigara BS (2010) Electrocatalytic oxidation of dopamine on acrylamide modified carbon paste electrode: a Voltammetric study. *Int J Electrochem Sci* 5:944–954
- Backe WJ, Yingling V, Johnson T (2014) The determination of acrylamide in environmental and drinking waters by large-volume injection - hydrophilic-interaction liquid chromatography and tandem mass spectrometry. *J Chromatogr A* 1334:72–78
- Elbashir AA, Omar MMA, Ibrahim WAW, Schmitz OJ, Aboul-Enein HY (2014) Acrylamide analysis in food by liquid chromatographic and gas chromatographic methods. *Crit Rev Anal Chem* 44:107–141
- Rashidi Nodeh H, Wan Ibrahim WA, Kamboh MA, Sanagi MM (2018) Magnetic graphene sol-gel hybrid as clean-up adsorbent for acrylamide analysis in food samples prior to GC-MS. *Food Chem* 239:208–216
- Bertuzzi T, Rastelli S, Mulazzi A, Pietri A (2017) Survey on acrylamide in roasted coffee and barley and in potato crisps sold in Italy by a LC-MS/MS method. *Food Addit Contam B* 10:292–299
- Abd El-Hady D, Albishri HM (2015) Simultaneous determination of acrylamide, asparagine and glucose in food using short chain methyl imidazolium ionic liquid based ultrasonic assisted extraction coupled with analyte focusing by ionic liquid micelle collapse capillary electrophoresis. *Food Chem* 188:551–558
- Wu J, Shen YD, Lei HT, Sun YM, Yang JY, Xiao ZL, Wang H, Xu ZL (2014) Hapten synthesis and development of a competitive indirect enzyme-linked immunosorbent assay for acrylamide in food samples. *J Agric Food Chem* 62:7078–7084
- Huang S, Lu S, Huang C, Sheng J, Zhang L, Su W, Xiao Q (2016) An electrochemical biosensor based on single-stranded DNA modified gold electrode for acrylamide determination. *Sens Actuat B-Chem* 224:22–30
- Liu C, Luo F, Chen D, Qiu B, Tang X, Ke H, Chen X (2014) Fluorescence determination of acrylamide in heat-processed foods. *Talanta* 123:95–100
- Hu Q, Xu X, Li Z, Zhang Y, Wang J, Fu Y, Li YB (2014) Detection of acrylamide in potato chips using a fluorescent sensing method based on acrylamide polymerization-induced distance increase between quantum dots. *Biosens Bioelectron* 54:64–71
- Ma XY, Guo ZZ, Mao ZQ, Tang YG, Miao P (2018) Colorimetric theophylline aggregation assay using an RNA aptamer and non-crosslinking gold nanoparticles. *Microchim Acta* 185(33)
- Ma CP, Wang FX, Wang XD, Han LZ, Jing H, Zhang H, Shi C (2017) A novel method to control carryover contamination in isothermal nucleic acid amplification. *Chem Commun* 53:10696–10699
- Mao JP, Lu YX, Chang N, Yang JE, Yang JC, Zhang SC, Liu YY (2016) A nanoplasmonic probe as a triple channel colorimetric sensor array for protein discrimination. *Analyst* 141:4014–4017
- Xie Y (2018) Colorimetric determination of Hg(II) via the gold amalgam induced deaggregation of gold nanoparticles. *Microchim Acta* 185:351
- Huang PC, Li JF, Liu X, Wu FY (2016) Colorimetric determination of aluminum(III) based on the aggregation of Schiff base-functionalized gold nanoparticles. *Microchim Acta* 183:863–869
- Du BB, Wang PL, Xiao C, Zhou Y, Wu L, Zhao H, Su XO, Yang J, He Y (2016) Antibody-free colorimetric determination of total aflatoxins by mercury(II)-mediated aggregation of lysine-functionalized gold nanoparticles. *Microchim Acta* 183:1493–1500
- Huo Y, Qi L, Lv XJ, Lai T, Zhang J, Zhang ZQ (2016) A sensitive aptasensor for colorimetric detection of adenosine triphosphate based on the protective effect of ATP-aptamer complexes on unmodified gold nanoparticles. *Biosens Bioelectron* 78:315–320
- Zhang YH, Wang YR, Zhu WX, Wang J, Yue XY, Liu W, Zhang DH, Wang JL (2017) Simultaneous colorimetric determination of bisphenol A and bisphenol S via a multi-level DNA circuit mediated by aptamers and gold nanoparticles. *Microchim Acta* 184:951–959
- Borghei YS, Hosseini M, Dadmehr M, Hosseinkhani S, Ganjali MR, Sheikhejad R (2016) Visual detection of cancer cells by colorimetric aptasensor based on aggregation of gold nanoparticles induced by DNA hybridization. *Anal Chim Acta* 904:92–97
- Hou YH, Wang JJ, Jiang YZ, Lv C, Xia L, Hong SL, Lin M, Zhang ZL, Pang DW (2018) A colorimetric and electrochemical immunosensor for point-of-care detection of enterovirus 71. *Biosens Bioelectron* 99:186–192
- Kumar D, Meenan BJ, Dixon D (2012) Glutathione-mediated release of Bodipy (R) from PEG cofunctionalized gold nanoparticles. *Int J Nanomedicine* 7:4007–4022

32. Kumar D, Mutreja I, Meenan BJ, Dixon D (2013) The profile of payload release from gold nanoparticles modified with a BODIPY (R)/PEG mixed monolayer. *J Nanopart Res* 25:16–30
33. Haiss W, Thanh NTK, Aveyard J, Fernig DG (2007) Determination of size and concentration of gold Nanoparticles from UV–Vis spectra. *Anal Chem* 79(11):4215–4221
34. Sun Z, Cui Z, Li H (2012) P-amino benzenesulfonic acid functionalized gold nanoparticles: synthesis, colorimetric detection of carbaryl and mechanism study by zeta potential assays. *Sens Actuat B-Chemical* 183:297–302
35. Flory PJ (1992) *Principles of polymer chemistry*, fifteenth printing. Cornell University press, New York, pp 246–256